Available online at www.sciencedirect.com
SCIENCE DIRECT®
Journal of Organometallic Chemistry 690 (2005) 4926–4932
Journal of Organometallic Chemistry
www.elsevier.com/locate/jorganchem

Synthesis and reactivity of organolanthanide complexes containing phenothiazine ligand toward carbodiimide and isothiocyanate

Liping Ma, Jie Zhang *, Ruifang Cai, Zhenxia Chen, Linhong Weng, Xigeng Zhou *

Department of Chemistry, Fudan University, Handan Road 220, Shanghai 200433, People's Republic of China

Received 14 July 2005; received in revised form 9 August 2005; accepted 10 August 2005
Available online 19 September 2005

Abstract

The synthesis and reactivity of new lanthanocene complexes incorporating phenothiazine ligand are described. The reaction of phenothiazine (HPtz) with ^{n}BuLi in THF and subsequently with 1 equiv. of $(C_5H_5)_2LnCl(THF)$ gave the original complexes $(C_5H_5)_2LnPtz(THF)$ (Ln = Yb(**1**), Er(**2**), Dy(**3**), Y(**4**)). Treatment of complexes **1**–**4** with *N*,*N*′-diisopropylcarbodiimide results in mono-insertion of carbodiimide into the Ln–N(Ptz)-bond to yield the corresponding guanidinates $(C_5H_5)_2Ln[(^{i}PrN)_2C(Ptz)]$ (Ln = Yb (**5**), Er (**6**), Dy (**7**), Y(**8**)). Further investigations indicate that phenyl isothiocyanate react with complexes **1** and **4**, giving the correspondent insertion products $(C_5H_5)_2Ln[SC(Ptz)NPh](THF)$ (Ln = Yb(**9**), Y(**10**)). All these complexes were characterized by elemental analysis and spectroscopic properties. The structures of complexes **2**, **5** and **9** were also determined by the X-ray single crystal diffraction analysis. All these reactions provide a new strategy for introducing a functional substituent at the nitrogen atom of phenothiazine via forming a new C–N(ring) bond.

Keywords: Organolanthanide; Insertion; Phenothiazine; Carbodiimide; Isothiocyanate

1. Introduction

Phenothiazines and Substituted phenothiazines are important biologically active heterocyclic compounds in which nitrogen and sulfur are incorporated in the tricyclic system. They are versatile compounds possessing anticholinergic, antihistamine, and antiemetic activities [1]. The coordination chemistry of metal ions with phenothiazine has been extensively investigated [2], and confirmed that phenothiazine–metal coordination complexes generally increased their antimutagenic activity, compared to their parent compounds. Recently, the coordination complexes of lanthanide nitrates with promethazine have also been reported [3].

Our recent research interests are in investigating the activity of the lanthanide–ligand bonds of organolanthanide derivates [4]. In the previous work, we studied the reactivity of some organolanthanide complexes containing the aromatic N-heterocyclic ligands toward carbodiimide, isocyanate or isothiocyanate [5]. The accumulated information indicates that the occurrence of the insertion strongly depends on the degree of the steric saturation around the center metal ion and the nature of the ligands. Continuing our recent investigation of the lanthanide–ligand insertion and learning more about the phenothiazine anion as a ligand, we herein report the synthesis of the organolanthanide phenothiazine complexes as well as their reactivity with carbodiimide and isothiocyanate, which provide an alternative strategy for introducing a functional substituent at the nitrogen atom of phenothiazine via forming a new C–N(ring) bond.

2. Results and discussion

2.1. Synthesis and characterization of lanthanocene phenothiazine complexes $(C_5H_5)_2LnPtz(THF)$ (Ln = Yb(1), Er(2), Dy(3), Y(4))

Lanthanocene amides are important organolanthanide complexes, and their synthesis and reactivity have received

* Corresponding author. Tel.: +86 21 65643885; fax: +86 21 65641740.
E-mail address: zhangjie@fudan.edu.cn (J. Zhang).

0022-328X/$ - see front matter © 2005 Elsevier B.V. All rights reserved.
doi:10.1016/j.jorganchem.2005.08.005

much attention. The metathesis and metalation reactions are the main routes for preparation of these complexes [6]. Here, we synthesized these organolanthanide phenothiazine complexes $(C_5H_5)_2LnPtz(THF)$ (Ln = Yb(**1**), Er(**2**), Dy(**3**), Y(**4**)) by the metathesis reaction of $(C_5H_5)_2LnCl(THF)$ with 1 equiv. of LiPtz in THF at room temperature, as shown in the following reaction equation

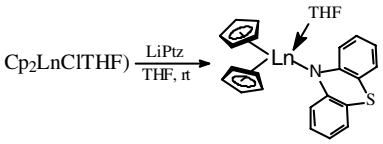

(1)

Ln = Yb(**1**), Er(**2**), Dy(**3**), Y(**4**)

Complexes **1**–**4** are air- and moisture-sensitive. They are soluble in THF and toluene and slightly soluble in *n*-hexane. Complexes **1**–**4** have been characterized by elemental analysis, IR and mass spectroscopy or ^1H NMR. In the IR spectra, complexes **1**–**4** exhibit two characterized absorptions at 1580 and 1560 cm^{-1}, which are attributed to the phenothiazine ligand, and two well-defined bands at 1070 and 880 cm^{-1} for the coordinated THF. The ^1H NMR of complex **4** also reveals that the solvent molecule THF is coordinated with the centre metal ion Y^{3+} in the solution. The crystal structure of **2** has been determinated by X-ray single crystal diffraction analysis. It also is the first crystallographically confirmed rare earth metal–phenothiazine compound. **2** Crystallized from the mixture solvent of THF and *n*-hexane at −20 °C in the monoclinic system, space group $P2_1/n$. The molecular structure of **2** is shown in Fig. 1. Selected bond lengths and angles are given in Table 1. Complex **2** is solvent monomer. The erbium atom is carried two η^5-cyclopentadienyl rings, one η^1-phenothiazine ligand and one coordinated THF. The coordination number of the central metal Er^{3+} is eight. The Er(1)–N(1) and Er(1)–O(1) distances (2.291(5), 2.349(5) Å) are in the normal ranges [7]. The Er–C(Cp) distances range from 2.622(7) to 2.663(8) Å. The average value of

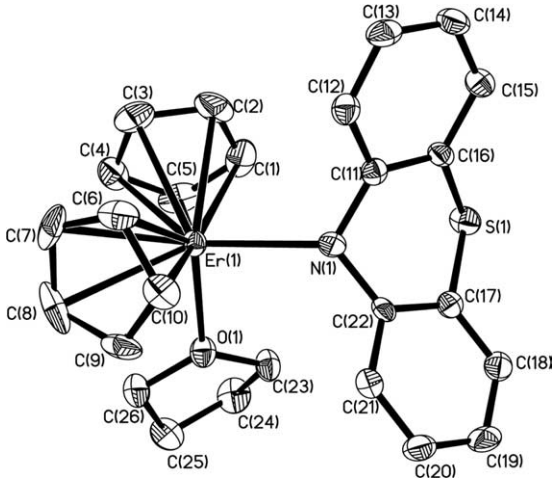

Fig. 1. ORTEP diagram of **2** with the probability ellipsoids drawn at the 30% level. Hydrogen atoms omitted for clarity.

Table 1
Selected bond lengths (Å) and angles (°) for **2**

Bond lengths (Å)	
Er(1)–N(1)	2.291(5)
Er(1)–O(1)	2.349(5)
Er(1)–C(6)	2.622(7)
Er(1)–C(4)	2.624(7)
Er(1)–C(3)	2.625(8)
Er(1)–C(9)	2.628(6)
Er(1)–C(5)	2.640(7)
Er(1)–C(8)	2.642(7)
Er(1)–C(7)	2.643(7)
Er(1)–C(10)	2.643(6)
Er(1)–C(1)	2.660(8)
Er(1)–C(2)	2.663(8)
S(1)–C(16)	1.760(7)
S(1)–C(17)	1.763(7)
N(1)–C(22)	1.406(8)
N(1)–C(11)	1.406(8)
Bond angles (°)	
N(1)–Er(1)–O(1)	94.22(17)
C(22)–N(1)–C(11)	115.1(5)
C(22)–N(1)–Er(1)	124.0(4)
C(11)–N(1)–Er(1)	118.3(4)

2.639(7) Å is similar to those found in other trivalent lanthanide complexes, such as $[Li(THF)_4]\{[(C_5H_5)_2ErH]_3Cl\}$, 2.65 Å [8a] and $(C_5H_5)ErCl_2(THF)_3$, 2.667 Å [8b].

2.2. Insertion of *N,N′*-diisopropylcarbodiimide into the Ln–N bond of complexes *1*–*4*

Our recently investigations have indicated that carbodiimide readily insert into the Ln–C or Ln–N-bonds of organolanthanide derivates, yielding the corresponding amidinate or guanidinate complexes [4c,4d,4e,5]. They provide an efficient method to synthesize the organolanthanide amidinate and guanidinate complexes. In order to study the effect of the nature of the organic nitrogen ligand on the insertion and explore the reactivity of complexes **1**–**4**, we first investigate the reaction of **1**–**4** with *N*,N′-diisopropylcarbodiimide. As shown in Scheme 1, when $^iPrN{=}C{=}N^iPr$ was added to a THF solution of **1**–**4** at room temperature, respectively, the corresponding guanidinate complexes $(C_5H_5)_2Yb[(^iPrN)_2C(Ptz)]$ (Ln = Yb(**5**), Er(**6**), Dy(**7**), Y(**8**)) were obtained in moderate yield, indicating that one carbodiimide molecule is inserted into the Ln–N(Ptz) bond.

The mass spectra of complexes **5**–**8** display the molecular ion peaks and the insertion fragments of $[(^iPrN)_2C(Ptz)]$. In IR spectra of these guanidinates, the characterized

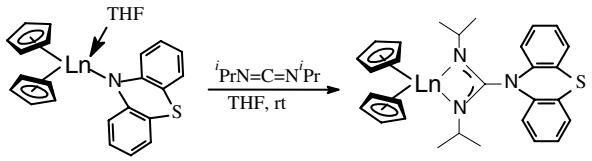

Ln = Yb(**1**), Er(**2**), Dy(**3**), Y(**4**) Ln = Yb(**5**), Er(**6**), Dy(**7**), Y(**8**)

Scheme 1.

absorption at ca. 2100 cm^{-1} for the ν_{as}(N=C=N) stretch of free carbodiimide is absent, but a new strong band at ca. 1660 cm^{-1} attributable to the delocalized –NCN– stretching mode is present [9]. The formation of the new ligand [(^{i}PrN)$_2$C(Ptz)] and solvent-free monomer structure of **8** have also been confirmed by the ^{1}H NMR. Complex **5** was further confirmed by the X-ray single crystal structural determination. The X-ray structure analysis results show that **5** (Fig. 2, Table 2) is a solvent-free monomer with the lanthanide atom bonded to two η^5-cyclopentadienyl rings and one chelating guanidinate ligand to form distorted tetrahedron geometry. As expected, the coordinated guanidinate group forms essentially a planar four-membered ring with the lanthanide atom within experimental errors. The bond angles around C(11) are consistent with sp^2 hybridization. The cent-Ln-cent (cent = the center of cyclopentadienyl ring) plane relative to the NCNLn plane is approximately perpendicular (88.6°). The C(11)–N(1) and C(11)–N(2) distances of the guanidinate group are approximately equivalent and significantly shorter than the C–N single bond distances, indicating that the π-electrons of the C=N double bond in the present structure are delocalized over the N–C–N unit [10]. Consistent with this observation, the Yb–N(1) and Yb–N(2) distances, 2.304(6) and 2.307(7) Å, are intermediate between the values observed for an Yb–N single bond distance and an Yb–N donor bond distances (2.19–2.69 Å) [9,11], and are comparable to the corresponding values found in (C_5H_5)$_2$Yb[(^{i}PrN)$_2$C(Cbz)] (Cbz = carbazolate) (Yb–Nav = 2.299(6) Å) [5]. The Yb–C(Cp) distances range from 2.570(11) to 2.600(10) Å, and are in the normal ranges observed for lanthanocene complexes. The average Yb–C(Cp) distance of 2.584(12) Å is similar to those found in other Cp_2Yb-containing compounds, such as (C_5H_5)$_2$Yb(PzMe$_2$)(HPzMe$_2$), 2.62(1) Å; [6j] [(C_5H_5)$_2$Yb(OCMe=C=CHMe)]$_2$, 2.63(1) Å; [12b] (C_5H_5)$_2$Yb(CH_3)(THF), 2.60(2) Å [12a].

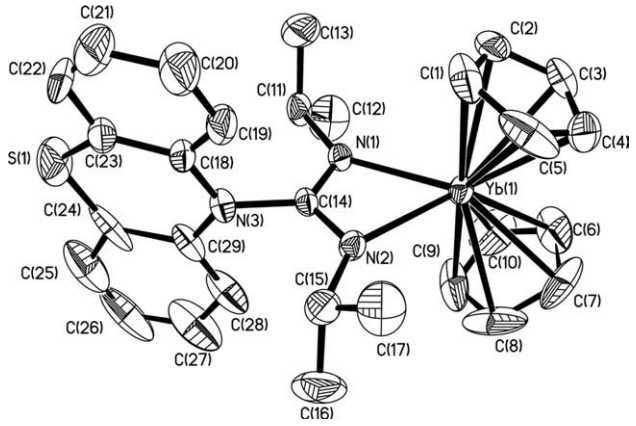

Fig. 2. ORTEP diagram of **5** with the probability ellipsoids drawn at the 30% level. Hydrogen atoms omitted for clarity.

Table 2
Selected bond lengths (Å) and angles (°) for **5**

Bond lengths (Å)	
Yb(1)–N(1)	2.304(6)
Yb(1)–N(2)	2.307(7)
Yb(1)–C(4)	2.570(11)
Yb(1)–C(6)	2.574(11)
Yb(1)–C(7)	2.576(12)
Yb(1)–C(9)	2.578(13)
Yb(1)–C(8)	2.584(12)
Yb(1)–C(1)	2.589(10)
Yb(1)–C(10)	2.590(12)
Yb(1)–C(3)	2.592(10)
Yb(1)–C(5)	2.598(12)
Yb(1)–C(2)	2.600(10)
S(1)–C(24)	1.686(17)
S(1)–C(23)	1.697(14)
N(1)–C(14)	1.312(10)
N(2)–C(14)	1.318(10)
N(3)–C(14)	1.453(10)
Bond angles (°)	
N(1)–Yb(1)–N(2)	58.0(2)
C(14)–N(1)–Yb(1)	92.8(5)
C(14)–N(2)–Yb(1)	92.5(5)
N(1)–C(14)–N(2)	116.6(7)
N(1)–C(14)–N(3)	121.8(7)
N(2)–C(14)–N(3)	121.6(7)
N(1)–C(14)–Yb(1)	58.2(4)
N(2)–C(14)–Yb(1)	58.4(4)
N(3)–C(14)–Yb(1)	177.2(6)
C(29)–N(3)–C(18)	124.7(8)
C(29)–N(3)–C(14)	117.0(8)
C(18)–N(3)–C(14)	117.2(7)

2.3. Reactions of complexes *1* and *4* with phenyl isothiocyanate

In order to gain more insight into the reactivity of complexes **1** and **4**, the reactions of **1** and **4** with phenyl isothiocyanate were also studied. It is found that reaction of complexes **1** and **4** with 1 equiv. of phenyl isothiocyanate result in the formation of the insertion product (C_5H_5)$_2$-Ln[SC(Ptz)NPh](THF) (Ln = Yb(**9**), Y(**10**)), respectively (Scheme 2). These compounds have been characterized by standard spectroscopic and analytical techniques. The structure of **9** has also been determinated by X-ray single crystal analysis.

X-ray determination indicates that complex **9** has a solvent monomer structure, as shown in Fig. 3, in which (C_5H_5)$_2$Yb fragment connects with one [SC(Ptz))NPh]$^-$ unit and one THF molecule. Its coordination geometry is similar to that in complex (C_5H_5)Yb(SC(Cbz)NPh)$_2$(THF) [5]. Selected bond distances and angles are given in Table 3. The N(1)–C(17) and S(1)–C(17) bond lengths, 1.327(7) and

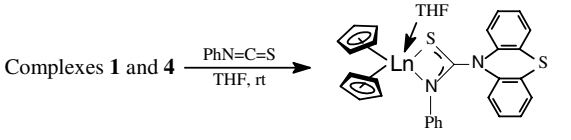

Scheme 2.

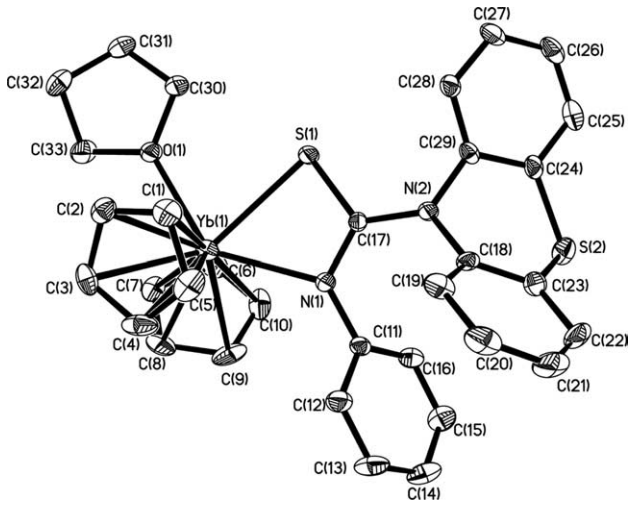

Fig. 3. ORTEP diagram of **9** with the probability ellipsoids drawn at the 30% level. Hydrogen atoms omitted for clarity.

1.725(6) Å, are in intermediate values between the corresponding C–N and C–S single- and double-bond distances [13]. These bond parameters indicate substantial electronic delocalization over the S–C–N unit [14]. Consistent with this, the observed Yb–N(1) (2.449(5) Å) bond distance is in agreement with that of the Yb–N(1) (2.515(3) Å) in $(C_5H_5)Yb(SC(Cbz)NPh)_2(THF)$. The Yb(1)–S(1) distance of 2.733(4) Å in **9** is comparable to the corresponding values found in $[(CH_3C_5H_4)_2Y(SC(NPh_2)NPh)]_2$ (Y–S 2.988(8) Å) [14], if the difference in ionic radii is considered [15]. Significantly, the distance of N(2)–C(17) (1.395(7) Å) in **9** is shorter than the corresponding value found in **5** (N(3)–C(14) 1.454(10) Å), which maybe indicted that the lone pair electrons of the N(2) atom partially delocalized on the S–C–N unit. The Yb–C(Cp) distances in complex **9** are the normal ranges observed for yetterbocene complexes [13].

Table 3
Selected bond lengths (Å) and angles (°) for **9**

Bond lengths (Å)	
Yb(1)–N(1)	2.449(5)
Yb(1)–O(1)	2.457(4)
Yb(1)–S(1)	2.733(4)
Yb(1)–C(10)	2.611(7)
Yb(1)–C(9)	2.624(7)
Yb(1)–C(4)	2.638(7)
Yb(1)–C(3)	2.644(7)
Yb(1)–C(6)	2.648(6)
Yb(1)–C(1)	2.652(6)
Yb(1)–C(2)	2.659(7)
Yb(1)–C(8)	2.660(6)
Yb(1)–C(5)	2.663(7)
Yb(1)–C(7)	2.668(6)
S(1)–C(17)	1.725(6)
S(2)–C(23)	1.758(8)
S(2)–C(24)	1.771(7)
N(1)–C(17)	1.327(7)
N(2)–C(17)	1.395(7)
N(2)–C(29)	1.437(7)
N(2)–C(18)	1.445(7)
Bond angles (°)	
N(1)–Yb(1)–O(1)	137.12(15)
C(17)–S(1)–Yb(1)	81.97(18)
C(17)–N(1)–Yb(1)	102.2(3)
C(17)–N(2)–C(29)	123.9(4)
C(17)–N(2)–C(18)	121.8(4)
C(29)–N(2)–C(18)	114.3(4)
N(1)–C(17)–N(2)	124.3(5)
N(1)–C(17)–S(1)	115.7(4)
N(2)–C(17)–S(1)	120.0(4)
N(1)–C(17)–Yb(1)	52.4(3)
N(2)–C(17)–Yb(1)	173.0(4)
S(1)–C(17)–Yb(1)	63.60(17)

3. Conclusion

We synthesized four new organolanthanide complexes containing the phenothiazine ligand and investigated the reactivity of them toward carbodiimide or isothiocyanate. These results indicate that *N*,*N*′-diisopropylcarbodiimide readily mono-insert into the lanthanide–nitrogen bonds of them under mild conditions, giving the corresponding guanidinates. Further study reveals phenyl isothiocyanate also react with complexes **1** and **4** to yield the insertion products. All the reactions provide an alternative synthetic strategy for the modification of the phenothiazine ligand.

3.1. Experimental

3.1.1. General procedure

All operations involving air- and moisture-sensitive compounds were carried out under an inert atmosphere of purified argon or nitrogen using standard Schlenk techniques. The solvents of THF, toluene, *n*-hexane were refluxed and distilled over sodium benzophenone ketyl under nitrogen immediately prior to use. $(C_5H_5)_2LnCl(THF)$ were prepared by the literature procedure [16]. Phenothiazine, *N*,*N*′-diisopropylcarbodiimide and phenyl isothiocyanate were purchased from Aldrich and were used without purification. Elemental analyses for C, H and N were carried out on a Rapid CHN-O analyzer. Infrared spectra were obtained on a NICOLET FT-IR 360 spectrometer with samples prepared as Nujol mulls. Mass spectra were recorded on a Philips HP5989A instrument operating in EI mode. Crystalline samples of the respective complexes were rapidly introduced by the direct inlet techniques with a source temperature of 200 °C. The values of *m*/*z* refer to the isotopes ^{12}C, ^{1}H, ^{14}N, ^{16}O, ^{89}Y, ^{164}Dy, ^{166}Er and ^{174}Yb. ^{1}H NMR data were obtained on a Bruker DMX-500 NMR spectrometer and were referenced to residual aryl protons in C_6H_6 (δ 7.16).

3.1.2. Synthesis of $(C_5H_5)_2YbPtz(THF)$ (**1**)

A solution of ^{n}BuLi (1.60 M, 1.10 mL in cyclohexane) was added dropwise to a 20 ml THF solution of HPtz (0.350 g, 1.76 mmol) at −30 °C. After stirred for 30 min at the low temperature, the mixture solution was slowly warmed to room temperature and stirred for 3 h. The reaction mixture was slowly added dropwise to the THF

solution of Cp_2YbCl (0.598 g, 1.76 mmol) at room temperature and the solution color soon turned from orange to dark green. After stirring for 12 h, the solvent was removed under vacuum and the solid residue was extracted with 30 ml toluene. The extract solution was concentrated and cooled at −20 °C to give dark green powder. Recrystallization of the powder from the mixture solvent of THF and toluene gave **1** as dark green crystals. Yield: 0.788 g (78%). Anal. Calc. for $C_{26}H_{26}NOSYb$, $M_w = 573.61$: C, 54.44; H, 4.57; N, 2.44. Found: C, 54.37; H, 4.51; N, 2.50%. IR (Nujol, cm^{-1}): 3545 w, 3339 w, 1582 s, 1560 s, 1440 s, 1429 s, 1288 s, 1228 s, 1211 s, 1074 m, 1010 s, 934 m, 875 m, 844 s, 780 s, 757 s, 665 w. EI-MS: *m/z* [fragment, relative intensity (%)] = 502 (M − THF, 98), 304 (M − THF − L, 84), 199 (L + H, 100), 65 (Cp, 10) [L = Ptz].

3.1.3. Synthesis of $(C_5H_5)_2ErPtz(THF)$ (2)

^{n}BuLi (1.60 M, 0.90 mL in cyclohexane) was added to a solution of HPtz (0.306 g, 1.54 mmol) in 30 ml THF at −30 °C. After being stirred for 3 h, the mixture solution was added to the THF solution of Cp_2ErCl (0.510 g, 1.54 mmol) at room temperature. The reaction mixture was subsequently worked up by the method described above. Pink crystals of **2** were obtained in 72% yield, 0.629 g. Anal. Calc. for $C_{26}H_{26}NOSEr$, $M_w = 567.80$: C, 55.00; H, 4.62; N, 2.47. Found: C, 54.91; H, 4.60; N, 2.52%. IR (Nujol, cm^{-1}): 3550 w, 3341 w, 1582 s, 11562 s, 1441 s, 1428 s, 1291 s, 1231 s, 1214 s, 1070 m, 1009 s, 934 w, 890 m, 843 s, 785 s, 756 s. EI-MS: *m/z* [fragment, relative intensity (%)] = 494 (M − THF, 55), 296 (M − THF − L, 100), 199 (L + H, 61), 65 (Cp, 16) [L = Ptz].

3.1.4. Synthesis of $(C_5H_5)_2DyPtz(THF)$ (3)

Following the procedure described for **1**, reaction of HPtz (0.382 g, 1.92 mmol) with ^{n}BuLi (1.60 M, 1.20 mL in cyclohexane) and subsequently with Cp_2DyCl (0.633 g, 1.92 mmol) gave **3** as pale yellow crystals. Yield: 0.736 g (68%). Anal. Calc. for $C_{26}H_{26}NOSDy$, $M_w = 563.07$: C, 55.46; H, 4.65; N, 2.49. Found: C, 55.42; H, 4.60; N, 2.54%. IR (Nujol, cm^{-1}): 3551 w, 3342 w, 1584 s, 1561 s, 1442 s, 1429 s, 1292 s, 1231 s, 1212 s, 1074 m, 1010 s, 933 w, 878 m, 847 s, 783 s, 759 s. EI-MS: *m/z* [fragment, relative intensity (%)] = 492 (M − THF, 13), 294 (M − THF − L, 100), 199 (L + H, 36), 65 (Cp, 12) [L = Ptz].

3.1.5. Synthesis of $(C_5H_5)_2YPtz(THF)$ (4)

Following the procedure described for **1**, reaction of HPtz (0.244 g, 1.23 mmol) with ^{n}BuLi (1.60 M, 0.62 mL in cyclohexane) and subsequently with Cp_2YCl (0.312 g, 1.23 mmol) gave **4** as pale yellow crystals. Yield: 0.433 g (72%). Anal. Calc. for $C_{26}H_{26}NOSY$, $M_w = 489.48$: C, 63.80; H, 5.35; N, 2.86. Found: C, 63.71; H, 5.37; N, 2.84%. IR (Nujol, cm^{-1}): 3555 w, 3340 w, 1597 s, 1572 s, 1444 s, 11342 s, 1313 s, 1244 s, 1070 m, 1011 s, 926 w, 860 m, 847 s, 793 s, 753 s, 664 w. ^{1}H NMR: δ 6.56–6.85 (m, 8H, $C_{12}H_8NS$), 6.10 (s, 10H, C_5H_5), 3.57 (m, 4H, $O(CH_2)_2(CH_2)_2$), 1.41 (m, 4H, $O(CH_2)_2(CH_2)_2$). EI-MS: *m/z* [fragment, relative intensity (%)] = 417 (M − THF, 43), 219 (M − THF − L, 67), 199 (L + H, 100), 65 (Cp, 26) [L = Ptz].

3.1.6. Synthesis of $(C_5H_5)_2Yb[(^iPrN)_2C(Ptz)]$ (5)

To a 30 mL THF solution of **1** (0.645 g, 1.12 mmol), *N*,*N*′-diisopropylcarbodiimide (0.141 g, 1.12 mmol) was slowly added dropwise at room temperature and stirred for several hours. The dark green solution became yellow-orange. After stirring for overnight, the reaction solution was concentrated by reduced pressure to about 2 mL. Addition of 20 mL of *n*-hexane resulted in the precipitation of a yellow solid. The resulting mixture was centrifuged, and the solution decanted. The precipitate was dried under vacuum to afford a yellow power. Recrystallization of the powder from the mixture solvent of THF and *n*-hexane gave **4** as yellow crystals. Yield: 0.457 g (65%). Anal. Calc. for $C_{29}H_{32}N_3SYb$, $M_w = 627.68$: C, 55.49; H, 5.14; N, 6.69. Found: C, 55.44; H, 5.10; N, 6.77. IR (Nujol, cm^{-1}): 3366 w, 1663 s, 1597s, 1573 s, 1312 m, 1245 s, 1172 m, 1093 s, 1014 s, 971 s, 772 s, 741 s, 663 w. EI-MS: *m/z* [fragment, relative intensity (%)] = 628 (M, 5), 502 (M − ^{i}PrNCN^{i}Pr, 19), 334 (L, 46), 304 (Cp_2Yb, 11), 199 (Ptz + H, 20), 65 (Cp, 9) [L = (^{i}PrN)$_2$C(Ptz)].

3.1.7. Synthesis of $(C_5H_5)_2Er[(^iPrN)_2C(Ptz)]$ (6)

Following the procedure described for **4**, reaction of **2** (0.534 g, 0.94 mmol) with *N*,*N*′-diisopropylcarbodiimide (0.119 g, 0.94 mmol) gave **5** as pink crystals. Yield: 0.433 g (74%). Anal. Calc. for $C_{29}H_{32}N_3Ser$, $M_w = 621.92$: C, 56.01; H, 5.19; N, 6.76. Found: C, 55.93; H, 5.10; N, 6.81%. IR (Nujol, cm^{-1}): 3363 w, 1660 s, 1591s, 1572 s, 1313 m, 1255 s, 1172 m, 1093 s, 1013 s, 924 w, 772 s, 741 s, 658 w. EI-MS: *m/z* [fragment, relative intensity (%)] = 496 (M − ^{i}PrNCN^{i}Pr, 66), 422 (M − Ptz, 40), 296 (Cp_2Er, 100), 199 (Ptz + H, 52), 66 (Cp + H, 15) [L = (^{i}PrN)$_2$C(Ptz)].

3.1.8. Synthesis of $(C_5H_5)_2Dy[(^iPrN)_2C(Ptz)]$ (7)

Following the procedure described for **4**, reaction of **3** (0.574 g, 1.02 mmol) with *N*,*N*′-diisopropylcarbodiimide (0.129 g, 1.02 mmol) gave **6** as pale yellow crystals. Yield: 0.415 g (66%). Anal. Calc. for $C_{29}H_{32}N_3SDy$, $M_w = 617.16$: C, 56.44; H, 5.23; N, 6.81. Found: C, 56.38; H, 5.26; N, 6.88%. IR (Nujol, cm^{-1}): 3365 w, 1660 s, 1594s, 1572 s, 1316 m, 1244 s, 1168 m, 1094 s, 1009 s, 952 s, 770 s, 736 s, 684 w. EI-MS: *m/z* [fragment, relative intensity (%)] = 618 (M, 7), 492 (M − ^{i}PrNCN^{i}Pr, 91), 420 (M − Ptz, 36), 294 (Cp_2Dy, 100), 198 (Ptz, 50), 65 (Cp, 10) [L = (^{i}PrN)$_2$C(Ptz)].

3.1.9. Synthesis of $(C_5H_5)_2Y[(^iPrN)_2C(Ptz)]$ (8)

Following the procedure described for **5**, reaction of **4** (0.764 g, 1.56 mmol) with *N*,*N*′-diisopropylcarbodiimide (0.197 g, 1.56 mmol) gave **8** as pale yellow crystals. Yield: 0.534 g (63%). Anal. Calc. for $C_{29}H_{32}N_3SY$, $M_w = 543.57$:

C, 64.08; H, 5.93; N, 7.73. Found: C, 63.95; H, 5.86; N, 7.88%. IR (Nujol, cm^{-1}): 3399 w, 1659 s, 1595s, 1573 w, 1506 s, 1389 s, 1340 s, 1317s, 1203 m, 1094 s, 1011 s, 953 s, 774 s, 740 s, 681 w. ^1H NMR: δ 6.49–6.76 (m, 8H, $C_{12}H_8NS$), 6.20 (s, 10H, C_5H_5), 4.06 (m, 1H, CH_3CHCH_3), 3.88 (m, 1H, CH_3CHCH_3), 1.13 (b, 6H, CH_3CHCH_3), 0.96 (b, 6H, CH_3CHCH_3). EI-MS: *m/z* [fragment, relative intensity (%)] = 543 (M, 44), 417 (M − ^{i}PrNCN^{i}Pr, 39), 334 (L, 57), 219 (Cp_2Y, 61), 199 (Ptz + H, 23), 65 (Cp, 13) [L = (^{i}PrN)$_2$C(Ptz)].

3.1.10. Synthesis of $(C_5H_5)_2Yb[SC(Ptz)NPh](THF)$ (9)

To a 20 mL THF solution of **1** (0.711 g, 1.24 mmol), phenyl isocyanate (0.156 g, 1.24 mmol) was slowly added dropwise at −30 °C. After stirred for 30 min at the low temperature, the mixture solution was slowly warmed to room temperature and stirred for several hours. All volatile substances were removed under vacuum to give a yellow powder. Further crystallization by diffusion of *n*-hexane into the above solution yielded the yellow crystals **7**. Yield: 0.492 g (56%). Anal. Calc. for $C_{33}H_{31}N_2OS_2Yb$, M_w = 708.76: C, 55.92; H, 4.41; N, 3.95. Found: C, 55.89; H, 4.37; N, 3.96%. IR (Nujol, cm^{-1}): 3358 w, 1587 s, 1302 m, 1277 s, 1248 s, 1197 m, 1152 s, 1068 s, 1015 s, 898 m, 869 m, 781 s, 759 s, 690 s, 669 w. EI-MS: *m/z* [fragment, relative intensity (%)] = 637 (M − THF, 4), 502 (M − THF − PhNCS, 49), 439 (M − THF − Ptz, 2), 304 (Cp_2Yb, 41), 199 (Ptz + H, 85), 135 (PhNCS, 65), 72 (THF, 50), 65 (Cp, 13).

3.1.11. Synthesis of $(C_5H_5)_2Y[SC(Ptz)NPh](THF)$ (10)

Following the procedure described for **5**, reaction of **4** (0.690 g, 1.41 mmol) with phenyl isothiocyanate (0.168 g, 1.41 mmol) gave **10** as pale yellow crystals. Yield: 0.590 g (67%). Anal. Calc. for $C_{33}H_{31}N_2OS_2Y$, M_w = 624.67: C, 63.45; H, 5.00; N, 4.48. Found: C, 63.37; H, 4.93; N, 4.54%. IR (Nujol, cm^{-1}): 3361 w, 3340 w, 1591 s, 1510w, 1361 m, 1279 m, 1250 s, 1142 s, 1069 s, 1016 s, 897 m, 869 m, 760 s, 690 s, 664 w. ^1H NMR: δ 7.00–7.60 (m, 5H, C_6H_5), 6.50–6.89 (m, 8H, $C_{12}H_8NS$), 3.55 (m, 4H, $O(CH_2)_2(CH_2)_2$), 1.37 (m, 4H, $O(CH_2)_2(CH_2)_2$). EI-MS: *m/z* [fragment, relative intensity (%)] = 552 (M − THF, 23), 417 (M − THF − PhNCS, 34), 229 (Cp_2Y, 56), 199 (Ptz + H, 100), 135 (PhNCS, 89), 72 (THF, 68), 65 (Cp, 24).

3.1.12. X-ray data collection, structure determination and refinement

Suitable single crystals of complexes **2**, **5** and **9** were sealed under argon in Lindemann glass capillaries for X-ray structural analysis. Diffraction data were collected

Table 4
Crystal and data collection parameters of complexes **2**, **5** and **9**

	2	**5**	**9**
Formula	$C_{26}H_{26}NOSEr$	$C_{29}H_{32}N_3SYb$	$C_{33}H_{31}N_2OS_2Yb$
Molecular weight	567.80	627.68	708.76
Crystal color	Pink	Orange-yellow	Orange-yellow
Crystal dimensions (mm)	0.20 × 0.15 × 0.10	0.20 × 0.20 × 0.15	0.40 × 0.25 × 0.20
Crystal system	Monoclinic	Monoclinic	Monoclinic
Space group	$P2_1/n$	$P2_1/n$	$P2_1/n$
Unit cell dimensions			
a (Å)	8.317(2)	9.503(4)	7.992(3)
b (Å)	17.180(4)	8.571(4)	16.514(6)
c (Å)	15.377(4)	32.851(13)	21.934(8)
β (°)	92.488(4)	94.841(5)	92.917(5)
V (Å^3)	2194.9(9)	2666.0(18)	2891.0(18)
Z	4	4	4
D_c (g cm^{-3})	1.718	1.564	1.628
μ (mm^{-1})	3.936	3.608	3.408
$F(000)$	1124	1252	1412
Radiation (λ = 0.710730 Å)	Mo Kα	Mo Kα	Mo Kα
Temperature (K)	298.2	293.2	293.2
Scan type	$\omega - 2\theta$	$\omega - 2\theta$	$\omega - 2\theta$
θ range (°)	1.78–26.01	2.19–25.01	1.54–25.01
h, k, l range	$-10 \leqslant h \leqslant 10$, $-21 \leqslant k \leqslant 12$, $-18 \leqslant l \leqslant 18$	$-11 \leqslant h \leqslant 11$, $-10 \leqslant k \leqslant 10$, $-39 \leqslant l \leqslant 28$	$-9 \leqslant h \leqslant 8$, $-19 \leqslant k \leqslant 19$, $-26 \leqslant l \leqslant 25$
Number of reflections measured	9944	10772	11941
Number of unique reflections [R_{int}]	4316 [0.0598]	4688 [0.0373]	5094 [0.0274]
Completeness to θ	99.7% (θ = 26.01)	99.8% (θ = 25.01)	99.6% (θ = 25.01)
Maximum and minimum transmission	0.6934 and 0.5065	0.6137 and 0.5323	0.5489 and 0.3426
Refinement method	Full-matrix least-squares on F^2	Full-matrix least-squares on F^2	Full-matrix least-squares on F^2
Data/restraints/parameters	4316/0/271	4688/0/307	5094/0/352
Goodness-of-fit on F^2	0.969	1.268	1.045
Final R indices [$I > 2\sigma(I)$]	R_1 = 0.0416, wR_2 = 0.0638	R_1 = 0.0595, wR_2 = 0.1138	R_1 = 0.0414, wR_2 = 0.1217
R indices (all data)	R_1 = 0.0849, wR_2 = 0.0738	R_1 = 0.0700, wR_2 = 0.1174	R_1 = 0.0502, wR_2 = 0.1273
Largest difference peak and hole (e Å^{-3})	1.030 and −0.583	1.607 and −2.186	1.698 and −0.825

on a Bruker SMART Apex CCD diffractometer using graphite-monochromated Mo Kα ($\lambda = 0.71073$ Å) radiation. During the intensity data collection, no significant decay was observed. The intensities were corrected for Lorentz-polarization effects and empirical absorption with SADABS program [17]. The structures were solved by the direct method using the SHELXL-97 program [18]. All non-hydrogen atoms were found from the difference Fourier syntheses. The H atoms were included in calculated positions with isotropic thermal parameters related to those of the supporting carbon atoms, but were not included in the refinement. All calculations were performed using the Bruker SMART program. A summary of the crystallographic data and selected experimental information is given in Table 4.

4. Supplementary data

Crystallographic data (excluding structure factors) for the structures reported in this paper have been deposited with the Cambridge Crystallographic Data Centre as supplementary Publication Nos. CCDC-272484 (**2**), CCDC-272485 (**5**), and CCDC-272486 (**9**). Copies of the data can be obtained free of charge on application to CCDC, 12 Union Road, Cambridge CB21EZ, UK (fax: +44 1223 336 033: e-mail: deposit@ccdc.cam.ac.uk).

Acknowledgments

We thank the National Natural Science Foundation of China and the Research Funds of Young Teacher of Fudan University for financial support.

References

[1] A.R. Katritzky, A.J. BoultonAdvances in Heterocyclic Chemistry, vol. 9, Academic Press, New York, 1968, p. 336.
[2] (a) B. Keshavan, J. Seetharamappa, Polyhedron 6 (1987) 465;
(b) R. Kroener, M.J. Heeg, E. Deutsch, Inorg. Chem. 27 (1988) 558;
(c) N.M. Made Gowda, L. Zhang, Synth. React. Inorg. Met–Org. Chem. 24 (1994) 831;
(d) N.M. Made Gowda, R.K. Vallabhaneni, I. Gajula, S. Ananda, J. Mol. Struct. 407 (1997) 125;
(e) B. Keshavan, H. Ramalingaiah, Transit. Met. Chem. 22 (1997) 185;
(f) B.J. Coe, J.A. Harris, L.J. Harrington, J.C. Jeffery, L.H. Rees, S. Houbrechts, A. Persoons, Inorg. Chem. 37 (1998) 3391;
(g) X. Zhang, Y. Xie, W. Yu, Q. Zhao, M. Jiang, Y. Tian, Inorg. Chem. 42 (2003) 3734.
[3] (a) B. Keshavan, P.G. Chandrashekara, N.M. Made Gowda, J. Mol. Struct. 553 (2000) 193;
(b) B. Keshavan, P.G. Chandrashekara, J. Ind. Chem. Soc. 76 (1999) 182.
[4] (a) J. Zhang, X.G. Zhou, R.F. Cai, L.H. Weng, Inorg. Chem. 44 (2005) 716;
(b) J. Zhang, L.P. Ma, R.F. Cai, L.H. Weng, X.G. Zhou, Organometallics 24 (2005) 738;
(c) J. Zhang, R.F. Cai, L.H. Weng, X.G. Zhou, Organometallics 23 (2004) 3303;
(d) J. Zhang, R.F. Cai, L.H. Weng, X.G. Zhou, J. Organomet. Chem. 672 (2003) 94;
(e) J. Zhang, R.Y. Ruan, Z.H. Shao, R.F. Cai, L.H. Weng, X.G. Zhou, Organometallics 21 (2002) 1420;
(f) X.G. Zhou, L.B. Zhang, M. Zhu, R.F. Cai, L.H. Weng, Z.X. Huang, Q.J. Wu, Organometallics 20 (2001) 5700.
[5] J. Zhang, R.F. Cai, L.H. Weng, X.G. Zhou, Organometallics 22 (2003) 5385.
[6] (a) R.E. Maginn, S. Manastyrskyj, M. Dubeck, J. Am. Chem. Soc. 85 (1963) 672;
(b) T.D. Tilley, R.A. Andersen, Inorg. Chem. 20 (1981) 3267;
(c) J.E. Bercaw, D.L. Davies, P.T. Wolczanski, Organometallics 5 (1986) 443;
(d) K.H. den Hann, J.L. de Boer, J.H. Teuben, A.L. Spek, B. Kojic-Prodic, G.R. Hays, R. Huis, Organometallics 5 (1986) 1726;
(e) S.P. Nolan, D. Stern, T.J. Marks, J. Am. Chem. Soc. 111 (1989) 7844;
(f) H. Schumann, P.R. Lee, J. Loebel, Chem. Ber. 122 (1989) 1897;
(g) W.J. Evans, R.A. Keyer, J.W. Ziller, Organometallics 12 (1993) 2618;
(h) M.A. Giardello, V.P. Conticello, L. Brard, M. Sabat, A.L. Rheingold, C.L. Stern, T.J. Marks, J. Am. Chem. Soc. 116 (1994) 10212;
(i) L. Mao, Q. Shen, M. Xue, J. Sun, Organometallics 15 (1997) 3711;
(j) X.G. Zhou, Z.E. Huang, R.F. Cai, L.B. Zhang, L.X. Zhang, X.Y. Huang, Organometallics 18 (1999) 4128.
[7] H. Schumann, P.R. Lee, J. Loebel, Chem. Ber. 123 (1990) 1331.
[8] (a) W.J. Evans, J.H. Meadows, A.L. Wayda, W.E. Hunter, J.L. Atwood, J. Am. Chem. Soc. 104 (1982) 2015;
(b) C.S. Day, V.W. Day, R.D. Ernst, S.H. Vollmer, Organometallics 1 (1982) 998.
[9] J.D. Wilkins, J. Organomet. Chem. 80 (1974) 349.
[10] R. Duchateau, A. Meetsma, J.H. Teuben, Organometallics 15 (1996) 1656.
[11] (a) X.G. Zhou, Z.E. Huang, R.F. Cai, L.X. Zhang, X.F. Hou, X.J. Feng, X.Y. Huang, J. Organomet. Chem. 563 (1998) 101;
(b) X.G. Zhou, H.Z. Ma, X.Y. Huang, X.Z. You, J. Chem. Soc., Chem. Commun. (1995) 2483;
(c) W.J. Evans, D.K. Drummond, L.A. Chamberlain, R.J. Doeden, S.G. Bott, H. Zhang, J.L. Atwood, J. Am. Chem. Soc. 110 (1988) 4983.
[12] (a) W.J. Evans, R. Dominguez, T.B. Hanusa, Organometallics 5 (1986) 263;
(b) X.G. Zhou, Z.Z. Wu, Z.S. Jin, J. Organomet. Chem. 431 (1992) 289.
[13] G. Hafelinger, Chem. Ber. 103 (1970) 2902.
[14] H. Li, Y. Yao, Q. Shen, L. Weng, Organometallics 21 (2002) 2529.
[15] A. Zalkin, T.J. Henly, R.A. Anderson, Acta Crystallogr Sect. C 43 (1987) 233.
[16] G. Wilkinson, J.M. Birmingham, J. Am. Chem. Soc. 78 (1956) 42.
[17] G.M. Sheldrick, SADABS, A Program for Empirical Absorption Correction, University of Göttingen, Germany, 1998.
[18] G.M. Sheldrick, SHELXL-97, Program for the Refinement of the Crystal Structure, University of Göttingen, Germany, 1997.